NRC Research Press

ARTICLE

Habitat suitability modeling based on a spatiotemporal model: an example for cusk in the Gulf of Maine

Jocelyn Runnebaum, Lisha Guan, Jie Cao, Loretta O'Brien, and Yong Chen

Abstract: Habitat use and distribution is a critical aspect in the management and conservation of a species, particularly for those in decline. Habitat suitability indices (HSI) are a common method of habitat mapping dependent on empirical data that can easily lead to misunderstanding the spatiotemporal dynamics of marine species experiencing population decline and density-dependent catchability within surveys. This is especially true when only a single monitoring program with limited spatiotemporal coverage is used. A delta-generalized linear mixed model was used to combine trawl and longline surveys to predict density estimates for cusk (*Brosme brosme*) in unsampled locations for use in HSIs. Catchability was estimated for longline and trawl gear without having an estimate of area fished for the longline survey. HSIs performed better using model-based density estimates from multiple surveys compared with sample-based abundance indices from a single survey. The increased spatial resolution can better inform the HSIs by providing information where the survey programs did not sample. This study provides a novel approach for integrating data from different monitoring programs for habitat modeling.

Résumé : L'utilisation et la répartition des habitats sont des aspects d'importance clé pour la gestion et la conservation des espèces, en particulier les espèces en déclin. Les indices de qualité de l'habitat (IQH) constituent une méthode répandue de cartographie des habitats qui repose sur de données empiriques pouvant facilement mener à une compréhension erronée de la dynamique spatiotemporelle d'espèces marines dont les populations sont en déclin et de la capturabilité dépendante de la densité dans les évaluations. Cela est particulièrement vrai quand une seule campagne de surveillance de couverture spatiotemporelle limitée est utilisée. Un modèle de mélange linéaire généralisé delta a été utilisé pour combiner des évaluations au chalut et à la palangre afin d'établir des estimations prévues de la densité pour le brosme (*Brosme brosme*) dans des emplacements non échantillonnés pour utilisation dans des IQH. La capturabilité a été estimée pour les palangres et les chaluts en l'absence d'estimation de la superficie pêchée pour l'évaluation à la palangre. Les IQH donnent de meilleurs résultats quand des estimations de la densité modélisées basées sur plusieurs évaluations sont utilisées, comparativement à des indices d'abondance basés sur les échantillons tirés d'une seule évaluation. La résolution spatiale accrue peut être avantageuse pour la détermination des IQH parce qu'elle fournit de l'information pour les emplacements non échantillonnés lors des campagnes d'évaluation. L'étude fournit une nouvelle approche d'intégration de données de différentes compagnes de surveillance pour la modélisation des habitats. [Traduit par la Rédaction]

Introduction

Habitat use and distribution is a critical aspect in the management and conservation of a species, particularly for those in decline. Habitat suitability indices (HSIs) are a method of assessing relative habitat quality for a species based on abundance at associated environmental conditions for a given location (Brooks 1997; Chen et al. 2009). The HSI can be projected spatially and temporally, providing valuable representation of changes in habitat quality over space and time and potential locations of a species' critical habitat (Chen et al. 2009). Such information is critical for implementing spatially explicit conservation management (Brooks 1997), evaluating shifts in habitat quality over time (Guan et al. 2017; Tanaka and Chen 2016), or understanding the impact of climate variability on suitable habitat distribution (Yu et al. 2016). Recent efforts have been made to improve the predictive capabilities of spatially projected HSIs (Tanaka and Chen 2015, 2016). However, these efforts do not address two critical shortcomings of conventional HSIs: (*i*) the abundance indices from survey catch data typically incorporated in these models do not account for changes in catchability over a time series; and (*ii*) the commonly used abundance indices, and therefore HSIs, are unable to incorporate surveys from multiple gear types that sample different segments of the population and likely cover different types of habitat. These issues need to be addressed to produce an unbiased evaluation of spatiotemporal changes in habitat quality for a species over its distributional range.

Conventional HSIs have been extensively applied to aquatic species by utilizing abundance indices derived from survey catch data (e.g., catch per unit effort, CPUE; Terrell 1984; Terrell and Carpenter 1997; Morris and Ball 2006). HSIs assume that high density of a species indicates high-quality habitat and that the absence or low density of a species indicates habitat of low value to the species. The use of catch data as a proxy for density assumes that sampled catches truly reflect the density or absence of a species at a given location and are not confounded by stock status, sampling inefficiency, and bias. This assumption may be reason-

Received 31 July 2017. Accepted 20 November 2017.

J. Runnebaum, J. Cao, and Y. Chen.* University of Maine, School of Marine Sciences, 5741 Libby Hall, Orono, ME 04469, USA.
L. Guan. University of Maine, School of Marine Sciences, 5741 Libby Hall, Orono, ME 04469, USA; Key Laboratory for Sustainable Utilization of Marine Fisheries, Ministry of Agriculture, Yellow Sea Fisheries Research Institute, Chinese Academy of Fishery Sciences, Qingdao 266071, China.
L. O'Brien. NOAA–NMFS, Northeast Fisheries Science Center, Woods Hole Laboratory,166 Water Street, Woods Hole, MA 02543, USA.
Corresponding author: Jocelyn Runnebaum (email: jocelyn.runnbeuam@maine.edu).
*Yong Chen currently serves as an Editor; peer review and editorial decisions regarding this manuscript were handled by Keith Tierney.

 Published at www.nrcresearchpress.com/cjfas on 20 December 2017.

able for species that have relatively constant and high survey catchability over space and time. However, for less-abundant species that are poorly sampled (e.g., low survey catchability or reside in habitat that is not well covered by the survey program) or for which survey catchability has changed over time, conventional HSIs may perform poorly or even produce biased results.

Conventional HSIs use available data from sampled locations, hereinafter referred to as sample-based HSIs, which are often restricted to the locations of occurrence and are typically processed to assume that the samples are representative (i.e., the species is effectively sampled) and are comparable through time (i.e., no changes in sampling distribution and efficiency). Therefore, the sample-based HSIs might not be appropriate in at least the following two situations: (*i*) the survey misses a major portion or type of the species' habitat; and (*ii*) sampling efficiency (i.e., catchability) changes over space and (or) through time due to density-dependent processes. Density-dependent habitat selection is a likely process for species in decline (MacCall 1990). When a species population is high, individuals move into previously marginal habitat because high-quality habitat is saturated; thus, the overall suitability of all occupied habitat declines on average (MacCall 1990). Conversely, as populations decline, individuals retreat to the highest suitable habitat as it becomes less densely occupied and available (MacCall 1990; Hare et al. 2012).

Another limitation of sample-based HSIs arise when data from multiple surveys are available for a species. Attempts to combine data from multiple surveys face serious difficulties, including quantifying the relative differences of catchability among different sampling gear (i.e., trawl and longline). Such complications often result in discarding data by trimming the survey data to common surveyed areas and time periods with consistent survey methods, utilizing probability of presence (Grüss et al. 2017; Brotons et al. 2004) or utilizing only one data set when multiples are available (Tanaka and Chen 2016). This is often unsatisfactory due to losses in spatial coverage given that different surveys of different gear types usually sample different areas or habitats. For example, trawl surveys likely do not sample rocky habitat as well as longline surveys. If rocky bottom is one of a species' preferred habitat types, using only trawl surveys for developing HSIs could bias the results.

Cusk (*Brosme brosme*) in the Gulf of Maine (GOM) is one species where assessment is difficult using conventional HSIs. It is a data-limited species, with low abundance and low catchability. Catchability of cusk is believed to have declined in the Northeast Fisheries Science Center (NEFSC) spring and fall bottom trawl surveys (BTS), presumably due to declines in stock abundance (Davies and Jonsen 2011; Hare et al. 2012), resulting in density-dependent catchability within the BTS. Additionally, changes to the survey protocols over the time series could influence the catchability of cusk in the BTS. In 2009, the BTS changed the sampling vessel, net type, and tow duration (Politis et al. 2014). The protocol changes in 2009 required the estimation of conversion coefficients for all species to allow for the data to be combined into a continuous time series (Miller et al. 2010). However, low catch numbers and low frequency of occurrence of cusk during the calibration study prevented conversion coefficients to be estimated for cusk (Miller et al. 2010). An operational stock assessment review in 2009 rejected the proposed analytical assessment and determined that a more representative index of abundance is needed for cusk (NEFSC 2013).

Declines in catch of cusk, and similar groundfish species, within the BTS prompted the development of the Northeast Fisheries Science Center (NEFSC) cooperative research bottom longline survey (LLS) in the western GOM to enhance monitoring efforts for data-poor and depleted stocks residing in rocky habitat to develop a more representative index of abundance (Hoey et al. 2013). The cusk population is now monitored by these two multispecies survey programs. These two survey programs differ in sampling efficiency, spatial coverage, and duration. Rocky, complex habitat, thought to be utilized by cusk (Collette and Klein-MacPhee 2002; Hare et al. 2012), is not well sampled by the BTS. However, the LLS is designed to sample rocky, complex bottom types more effectively than the BTS covering the same region, due to the nature of the gear. Both survey programs are stratified by depth and overlap in the western GOM.

In the case of cusk, the BTS would likely not provide a realistic evaluation of habitat quality because of catch declines over the time series and poor sampling in rocky habitat. Conventional habitat modeling based on either BTS or LLS would likely produce biased results. This study proposes a modeling framework for use with data-limited species such as cusk by combining the BTS and the bottom LLS data to derive model-based density estimates to improve spatial resolution of data for use in HSIs. The results from the model-based HSI are contrasted with those derived from sample-based HSI to test the hypothesis that HSI performance would improve with the use of higher resolution spatial information from combining multiple surveys and imputing values for unsampled locations.

Methods

Survey and environmental data

Data on cusk abundance are available from the NEFSC spring and fall BTS (1980–2015) and the NEFSC spring and fall bottom LLS (2014–2015). The BTS is a demersal, multispecies, depth-stratified random survey synoptic of the GOM and Georges Bank (GB) (Politis et al. 2014). The NEFSC developed a depth-stratified random LLS in the western and central GOM to better sample species that primarily reside in complex habitat (Hoey et al. 2013). Six survey strata were selected for the LLS from ten offshore and four inshore strata from the BTS. This survey also samples in the spring and fall to coincide with the BTS and randomly samples hard bottom sites within each stratum (Hoey et al. 2013). The LLS follows the tidal cycle, with gear deployed 1 h before slack tide and fished for 2 h. The longline gear is one nautical mile long (1 n.m. = 1.852 km), with 1000 semicircle hooks baited with squid set within a three-nautical mile grid (Hoey et al. 2013).

Environmental variables known to impact cusk habitat are depth, temperature, and sediment type (Hare et al. 2012). Cusk have been documented between 18 and 1000 m and are thought to tolerate temperatures between 0 and 14 °C, with the majority of cusk occurring between 6 and 10 °C in the GOM (Cohen et al. 1990; Collette and Klein-MacPhee 2002). Cusk are hypothesized to prefer rock, gravel, or pebble sediment, but are known to inhabit mud areas in the GOM, excluding smooth sand (Cohen et al. 1990; Collette and Klein-MacPhee 2002). These three environmental variables were used to develop HSIs for the GOM and GB regions.

Simulated bottom temperature data (1980–2013) were obtained from the Northeast Coastal Ocean Forecast System (NECOFS) integrated atmosphere–ocean model forecast system for the GOM, GB, and New England Shelf regions. The simulated temperature data were generated from an unstructured Finite-Volume Community Ocean Model grid for these regions (Beardsley et al. 2013; NECOFS 2013) and averaged over the primary 2 months when the surveys were conducted.

For sample-based HSIs, depth data from the BTS were used. For model-based HSIs, depth was extracted from the General Bathymetric Chart of the Oceans (GEBCO 2014) 30 arc-second interval grid. Sediment data were extracted from the United States Geological Survey (USGS) East-Coast Sediment Texture Database (Poppe et al. 2014) using geographic information system (GIS). In situ temperature data are not available for the model-based density estimates used in the HSI, since these come from model projections. To compare design-based and model-based HSIs, the same temperature data were used in both analyses to not confound results by developing HSIs from different types of temperature data (i.e., observed versus simulated). Additionally, a seasonal average can represent the environmental conditions a species would encounter during a season relative to an instantaneous temperature.

The study area was divided into 5710 cells (0.05° × 0.05°) for predicting grid-based densities, which were then used to develop model-based HSIs by season. Simulated environmental variables were assigned to the beginning of the trawl survey location for sample-based HSIs and to the center of 0.05° × 0.05° grid cells for model-based HSIs.

Spatial–temporal model for predicting species density

A spatiotemporal delta-generalized linear mixed model (delta-GLMM) initially developed by Thorson et al. (2015) was applied (using the VAST package in R; Thorson and Barnett 2017) to data collected from both NEFSC BTS and LLS to estimate cusk density for each season (i.e., spring and fall) from 1980 to 2015 to match the timing of simulated temperature data. This is a two-stage model that ultimately infers population density throughout the study area. Survey data are fit in two stages by: (1) estimating the probability of encountering and catching cusk (i.e., presence–absence) and then (2) estimating catches (C) when cusk are present (Thorson et al. 2015).

The first model component estimates the probability (p) of catching at least one of the target species:

$$\Pr[C > 0] = p \tag{1}$$

The second stage of the model approximates positive catches (c):

$$\Pr[C = c \mid C > 0] = \mathrm{Gamma}(c, \sigma^{-2}, \lambda\sigma^2) \tag{2}$$

The probability density function Gamma(c, x, y) is evaluated at c given a gamma distribution, where λ is the expected catch if encountered, and σ is the coefficient of variation for positive catches (Thorson and Ward 2014; Thorson et al. 2015).

Spatial autocorrelation is incorporated into the model as a random effect to account for the spatial dependence of species density. Two Gaussian Markov random fields are included in both stages of the model as a random effect to account for spatial (ω) and spatiotemporal (ε) autocorrelation (Thorson et al. 2015). The random fields are approximated at 250 prespecified knots that are generated based on the proportional density of survey data over the defined domain (i.e., the 0.05° × 0.05° grid; Thorson et al. 2015). The spatial (ω) and spatotemporal (ε) random effects were used in both spring and fall density estimates.

Encounter probability p and positive catch rates λ are approximated using linear predictors (Thorson et al. 2015):

$$p_i = \mathrm{logit}^{-1}\left[d_{T_{(i)}}^{(p)} + Q_i^{(p)} + \omega_{J_{(i)}}^{(p)} + \varepsilon_{J_{(i)},T_{(i)}}^{(p)}\right] \tag{3}$$

$$\lambda_i = w_i \exp\left[d_{T_{(i)}}^{(\lambda)} + Q_i^{(\lambda)} + \omega_{J_{(i)}}^{(\lambda)} + \varepsilon_{J_{(i)},T_{(i)}}^{(\lambda)}\right] \tag{4}$$

where p_i and λ_i are the expected probabilities of an occupied habitat and positive catches, respectively, given occupied habitat for sample i at a given location; $d_{T_{(i)}}$ is the mean reference density (encounters/positive catch rates) in year $T_{(i)}$; Q_i is catchability for each survey; w_i is the area swept for sample i; J_i is the nearest knot to sample i; $\omega_{J_{(i)}}$ is a random field accounting for spatially correlated variability at knot J_i that is persistent among years; and $\varepsilon_{J_{(i)},T_{(i)}}$ is the random field accounting for spatiotemporal correlation at knot J_i in year $T_{(i)}$ (Thorson et al. 2015). Spatial and spatial–temporal random fields were used in all models for both seasons.

A design matrix with indicator variables for each survey is used to estimate Q_i. This study assumes the need to estimate three catchability parameters due to the BTS protocol changes in 2009 and the inclusion of the LLS. A three-column design matrix was built using ThorsonUtilities with as many rows as observations and reduced to a two-column matrix for identifiability. The 2009 protocol changes cause the intercepts of Q_i and $d_{T_{(i)}}$ to be collinear due to a lack of variance in Q_i in a given year as a result of two nonoverlapping time blocks in the BTS. To resolve this issue, year effect was modeled via a temporal autocorrelation structure:

$$\beta_1(t+1) \sim \mathrm{Normal}\left[\rho_{\beta_1}(t), \sigma_{\beta_1}^2\right] \tag{5}$$

$$\beta_2(t+1) \sim \mathrm{Normal}\left[\rho_{\beta_2}(t), \sigma_{\beta_2}^2\right] \tag{6}$$

where ρ_{β_1} and ρ_{β_2} are defined as a random walk as specified in the model (Thorson 2017). Catchability is then removed from the model, and the underlying species density is predicted at each knot. Grid cells are assigned the density of the nearest knot based on closest Euclidean distance calculated using the Voronoi tool in the PBSmapping package in R (Schnute et al. 2015). Density fields are then extracted for each grid cell to use within the HSIs.

Within the delta-GLMM, catch rate was estimated as catch number by area swept (Thorson et al. 2015). Area swept for the BTS tows in the GOM has been standardized as 0.024 km² for the Bigelow and 0.038 km² for the Albatross IV and the Delaware II (NEFSC 2013). The area fished ($A_{i,y}$ km²) for the LLS is calculated as the distance between the beginning location of the longline and the end of the longline set (in km; L) times an estimated bait plume (b) along the length of the longline for each sample site (i) in a given year (y):

$$A_{i,y} = L_{i,y}b \tag{8}$$

The bait plume (b) is assumed to be a fixed constant (0.28 km) for all years and all locations. Evaluation of the impact of varying bait plume sizes on density estimates can be found in Appendix A.

Habitat suitability indices

HSIs quantify the overall habitat quality for a species by evaluating species density associated with each selected environmental variable. Suitability indices (SIs) quantify the relationship between an environmental variable and species abundance at a given location (Terrell 1984; Terrell and Carpenter 1997; Morris and Ball 2006). SIs are then combined either through a geometric mean (GMM) or an arithmetic mean (AMM) to derive an overall HSI to quantify habitat quality from relatively good (1) to relatively bad (0) (Chen et al. 2009; Tanaka and Chen 2016). HSIs assume that locations with the highest abundance have the highest quality habitat for that organism.

Season-specific HSIs were developed for 1980–2013 mean conditions using two different types of abundance indices to compare the performance of model-based HSIs relative to sample-based HSIs. CPUE (i.e., catch number per area swept) from the BTS was used as the abundance index for the sample-based HSIs. Model-based density estimates derived from both the BTS and LLS were extracted for each cell and used in the model-based HSIs. All abundance indices were calculated separately for spring (i.e., April–May) and fall (i.e., October–November). The time series for cusk used in this study is from 1980 to 2015; however, simulated monthly mean temperature data were only available up to 2013 at the time of writing. All data (i.e., observed CPUE and model-based density) were trimmed to 1980–2013 and averaged for the entire time series. NECOFS-simulated bottom temperatures (Chen et al. 2006) were averaged by season for the time series. Mean environmental data (i.e., bottom temperature, depth, and sediment type) were extracted for the beginning latitude and longitude for each trawl haul and for each grid center using GIS.

Fisher natural breaks were used to bin the continuous environmental variables of depth and bottom temperature (Bivand 2013; Tanaka and Chen 2016). Sensitivity analyses were conducted to determine both the most appropriate number of bins for each model and the minimum bin size (five to eight bins). Categorical sediment data were extracted from the USGS sediment layer, and the nine defined sediment types were used as bins (Poppe et al. 2014).

For the sample-based HSIs, CPUE for cusk was calculated as catch number at station (i), in season (s), and year (y) per area swept for each vessel (v) (Chang et al. 2012; Tanaka and Chen 2015, 2016):

$$(9) \qquad \mathrm{CPUE}_{isy} = \frac{\text{Catch Number}_{isy}}{\text{Area Swept}_{v}}$$

where catch number is the total number of cusk caught per tow, and area swept is standardized for each of the three vessels used in the BTS (NEFSC 2013). For model-based HSIs, mean abundances estimated from the spatiotemporal model were used for each $0.05° \times 0.05°$ grid cell. The SI for bin (b) of environmental variable (k), $\mathrm{SI}_{b,k}$, was calculated on a 0.0 to 1.0 scale (Chang et al. 2012; Tanaka and Chen 2015, 2016):

$$(10) \qquad \mathrm{SI}_{b,k} = \frac{\overline{\mathrm{CPUE}_{b,k}} - \overline{\mathrm{CPUE}}_{k,\min}}{\overline{\mathrm{CPUE}}_{k,\max} - \overline{\mathrm{CPUE}}_{k,\min}}$$

where $\overline{\mathrm{CPUE}_{b,k}}$ is the mean CPUE over all sampled stations within bin b for each environmental variable k (Tanaka and Chen 2015, 2016). These SI values were then averaged by an arithmetic mean (AMM) and a geometric mean (GMM):

$$(11) \qquad \mathrm{HSI}_{\mathrm{AMM}} = \frac{\sum_{i=1}^{n} \mathrm{SI}_k}{n}$$

$$(12) \qquad \mathrm{HSI}_{\mathrm{GMM}} = \prod_{i=1}^{n} \mathrm{SI}_k^{1/n}$$

where all SI_k represent equally weighted SI values for the kth environmental variable, and n is the number of environmental variables included.

The sample- and model-based HSIs were based on empirical data from the BTS and modeled density estimates, respectively. Owing to the limitation of sample-based HSI, the CPUE used was restricted to only the spring and fall BTS. However, model-based HSIs incorporated density estimates derived from both the BTS and LLS. Density estimates are extrapolated over the grid cells based on the abundance estimates for the nearest knot. The $0.05° \times 0.05°$ grid size was used to increase spatial resolution for environmental variables over the entire survey area.

Results

Spatial–temporal model for predicting species density

Varying estimates of area fished for the LLS were also tested to evaluate the relative impact of bait plumes on abundance estimates. The tested values of b to estimate area fished (i.e., 0.28, 0.56, 1.12 km) had no impact on density estimates and annual indices of abundance because the catchability coefficient could account for differences in catch rate (Appendix A). This makes it possible to combine two different gear types without needing to know the size of the bait plume for the LLS.

Density plots for annual species distribution indicate that the cusk population is densest in the central GOM, with annual variability (Fig. 1). Cusk density has constricted over the time period, with lower densities predicted inshore in both seasons later in the time series (Fig. 1). Cusk density is highest from 1980 to 1993 in the time series, with a slight decrease in density particularly in the offshore (yellow and red regions, Fig. 1). Cusk population density from 1994 to 2007 remains relatively constant in the spring and the fall. Starting in 2008 to the end of the time series, low density levels prevail, particularly in the inshore regions. Over the entire time series, density around GB (i.e., the southernmost extent of the plots) shows a steady decline in cusk abundance, predominately in the spring and somewhat in the fall (Fig. 1). Pearson residual plots suggest there is no significant spatiotemporal pattern in the residuals (Fig. 1).

HSI models

Sample-based HSI

Sample-based HSIs were derived from observed CPUE from the BTS using simulated temperature and sediment data and observed mean depths. Simulated seasonal mean bottom temperatures were compared with observed instantaneous bottom temperatures from the BTS when available (Fig. 2). The instantaneous observed temperatures were more variable (spring: 1.35 to 12.30 °C; fall: 4.47 to 19.20 °C) compared with simulated temperatures (spring: 4.29 to 7.64 °C; fall: 6.66 to 14.09 °C; Fig. 2). Observed mean depths were used to build sediment sample-based SIs. Observed depths were compared with simulated depths at the location of sampling and were more variable at deeper depths than at shallower depths but were well correlated (Fig. 3).

Assuming the simulated temperature represents mean conditions that cusk would experience during each season, the preferred mean temperatures for cusk were between 7.05 and 7.63 °C in the spring and 8.14 and 8.72 °C in the fall (Fig. 4). Cusk preferred depths between 189 and 224 m in the spring and 192 and 227 m in the fall (Fig. 4). Bedrock was the most preferred sediment type, followed by a combination of sand, silt, and clay in the spring sample-based HSI (Fig. 4) and combinations of clay, silt, and sand in the fall sample-based HSI (Fig. 4).

HSIs assume that habitat quality increases with density. A simple linear regression between abundance and HSI was used to test this assumption. Sample-based HSIs for the spring and fall did not show a clear relationship between density and habitat quality (Table 1). Linear regressions between CPUE and sample-based HSIs in the spring showed a significant relationship ($p < 0.01$), but the models failed to fit the data well (e.g., spring AMM, CPUE $R^2 < 0.072$; fall AMM, CPUE $R^2 < 0.05$; Table 1).

Model-based HSI

Model-based HSIs were derived from density field estimates from the delta-GLMM (spring and fall, $b = 0.28$ km). Model-based bottom temperature SI curves found 6.87 to 7.25 °C as the most suitable temperatures in the spring and 8.07 to 8.68 °C in the fall (Fig. 4). SI depth curves for abundance indices derived from both data sets showed that 161 to 208 m was the most preferred depth range in both the spring and fall. For all spring and fall model-based HSI models, the most preferred sediment type was a combination of sand, silt, and clay in both the spring and fall (Fig. 4).

Comparison between sample- and model-based HSIs

The model-based SI and sample-based SI curves are similar in both the spring and the fall, with the exception of sediment. Both the model-based and sampled-based bottom temperature SI curves indicate cusk were caught in slightly warmer waters in the fall but prefer temperatures around 7 °C in the spring and 8 °C in the fall (Fig. 4). The model-based depth SI curves showed cusk were associated with depth ranges between 2 and 877 m in the spring and fall compared to BTS observed depth ranges of 22 to 368 m in the spring and 20 to 412 m in the fall. Both model-based depth SI curves showed 161 to 208 m as the most preferred depth ranges in the spring and fall (Fig. 4). These preferred depth ranges are shallower than the preferred depth ranges estimated (189 to

Fig. 1. (Upper panels) Density field plots from the delta-generalized spatiotemporal model. Red indicates areas of higher abundance; blue indicates areas of lower abundance. (Lower panels) Pearson residual plots of the density field estimates from the delta-generalized spatiotemporal model. [Colour online.]

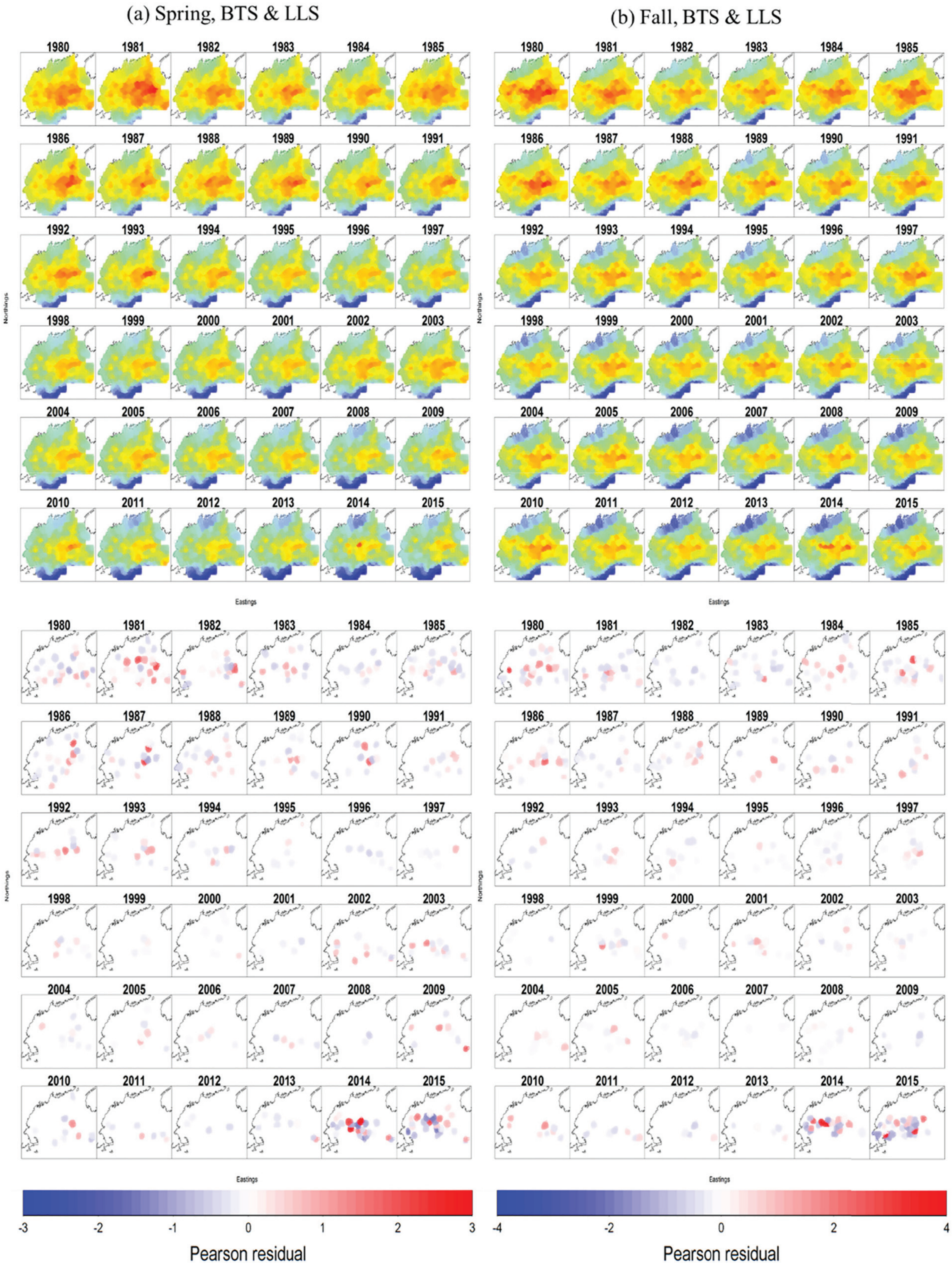

Fig. 2. Linear regression of simulated and observed mean seasonal bottom temperature (BT). Northeast Coastal Ocean Forecast System (NECOFS) simulated seasonal mean temperatures (*x* axis) are compared with instantaneous observed BT from the Northeast Fisheries Science Center (NEFSC) bottom trawl survey (BTS) (*y* axis), when recorded on the survey.

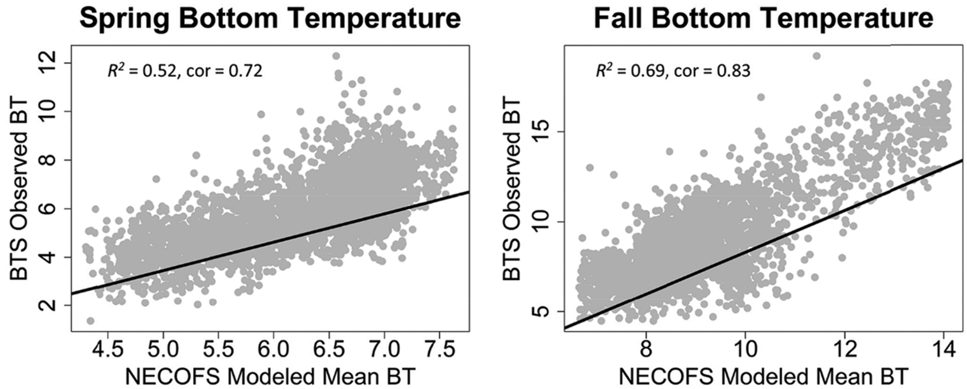

Fig. 3. Linear regression of simulated and observed mean depths. General Bathymetric Chart of the Oceans (GEBCO) simulated depths (*x* axis) are compared with mean observed bottom depths from the NEFSC BTS (*y* axis) recorded on the survey.

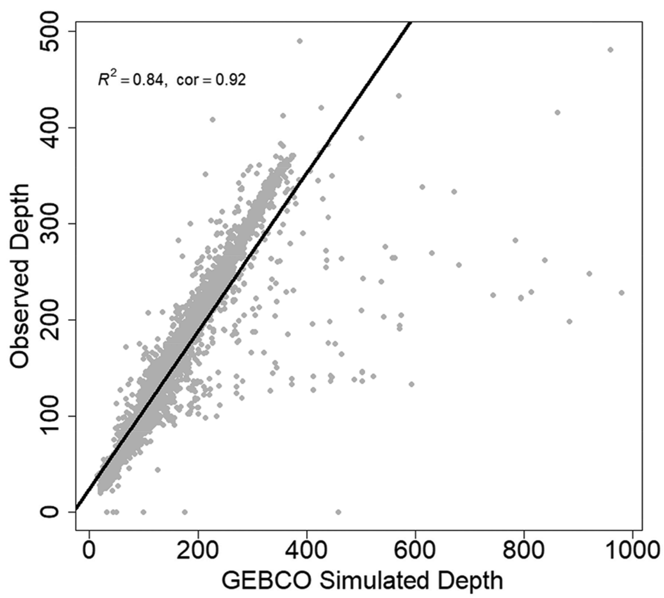

224 m in the spring and 192 to 227 m in the fall) by the sample-based depth SI, but show the same pattern of preferring deeper depths in the spring and shallower depths in the fall (Fig. 4). Pearson correlations (r) indicate temperature and depth were positively correlated in the spring for both model-based (r = 0.61) and sample-based (r = 0.28) HSIs and negatively correlated in the fall for model-based (r = –0.71) and sample-based HSIs (r = –0.31).

The model-based GMM HSIs had higher coefficient of determination (R^2) and correlation coefficients for both seasons in all models except in the fall sample-based HSI (Table 1). Model-based HSIs derived only from the BTS were statistically significant (p < 0.001) with an R^2 of 0.3836 (AMM) and 0.4366 (GMM) for the spring and 0.2927 (AMM) and 0.3041 (GMM) for the fall (Table 1, modeled BTS only). Model-based HSIs predicted habitat quality well relative to survey catch rates (Fig. 5).

The preferred range of each environmental variable for sample-based HSIs is limited by the sampling locations. The model-based sediment SI histograms derived for both the spring and fall indicated a mixture of sand, silt, and clay to be the most preferred sediment (Fig. 4). Most of the cusk catches in both the spring and fall BTS were in these sediment types (Fig. 6). For sample-based sediment, SI histograms indicated that bedrock was the most important sediment type in the spring and gravel the third most important for the fall (Fig. 4). However, for the entire time series (1980–2013), one cusk was caught in bedrock and two in gravel in the spring, and in the fall zero were caught in bedrock and six were caught in gravel (Fig. 6). Similarly, sample-based HSIs depicted a narrower depth range and preferred depth relative to model-based HSIs (Fig. 4). The NEFSC trawl survey sampling locations were shallower (e.g., 22–388 m in the spring and 20 to 516 m in the fall; Fig. 7) relative to simulated depths available to the model-based HSIs (i.e., 2 to 877 m).

The SI for each variable was removed to determine the relative importance of that variable to the overall HSI, the bigger the decrease in R^2 the more important that variable is to habitat suitability. For sample-based HSIs, temperature was the biggest driver in habitat suitability in the spring, while sediment was the biggest driver in the fall (Table 1). However, for the fall sample-based GMM HSI, the R^2 increased when depth was removed, indicating this variable is not important within that model potentially due to the negative correlation with temperature. For model-based HSIs, temperature was the biggest driver in the spring, and depth was the biggest driver in the fall (Table 1).

Discussion

Comparisons between model-based and sampled-based HSIs indicate that fully utilizing all available survey data changed the perception of depth and sediment preferences of cusk because of the imputed estimates for unsampled locations. Thus, model-based density estimates that incorporated data from multiple gear types can overcome the sampling bias of trawl surveys for species that associate with complex habitats. HSIs were better able to predict an increase in habitat quality with increasing density with the use of model-based abundance estimates (Table 1).

Spatial–temporal model for predicting species density

Bottom trawl surveys are likely to produce biased estimates of abundance if the species' spatial distribution has changed over time and if gear performance varies by the habitat that the target species associates with over time (Thorson et al. 2013; Kotwicki et al. 2014). The decline in the cusk population likely reduced catchability in the BTS due to the population constricting to rocky habitat not accessible to the BTS (Davies and Jonsen 2011; Hare et al. 2012), resulting in a decreased probability of successful sampling. Annual density field estimates and subsequent abundance indices (Appendix A) based only on the BTS are therefore likely biased due to density-dependent and time-varying catchability.

The LLS was incorporated into the model-based abundance estimates to compensate for density-dependent processes within

Fig. 4. Comparing model-based and sample-based suitability index (SI) curves for cusk. For these comparisons, (*a*) all model-based abundance SIs were derived from both bottom trawl surveys (BTS) and longline surveys (LLS); and (*b*) sample-based abundance SIs were derived from the BTS. Sediment types include bedrock (br), gravel (gr), gravelly sediment (gr-sd), sand (sd), 33% sand, silt, and clay (sd/st/cl), 25%–50% sand with clay and silt (sd-cl/st), >75% sand with silt and clay (sd-st/cl), 50%–75% clay with silt with sand (cl-st/sd), and clay (cl) (Poppe et al. 2014). Bottom temperature (BT) is measured in degrees Celsius.

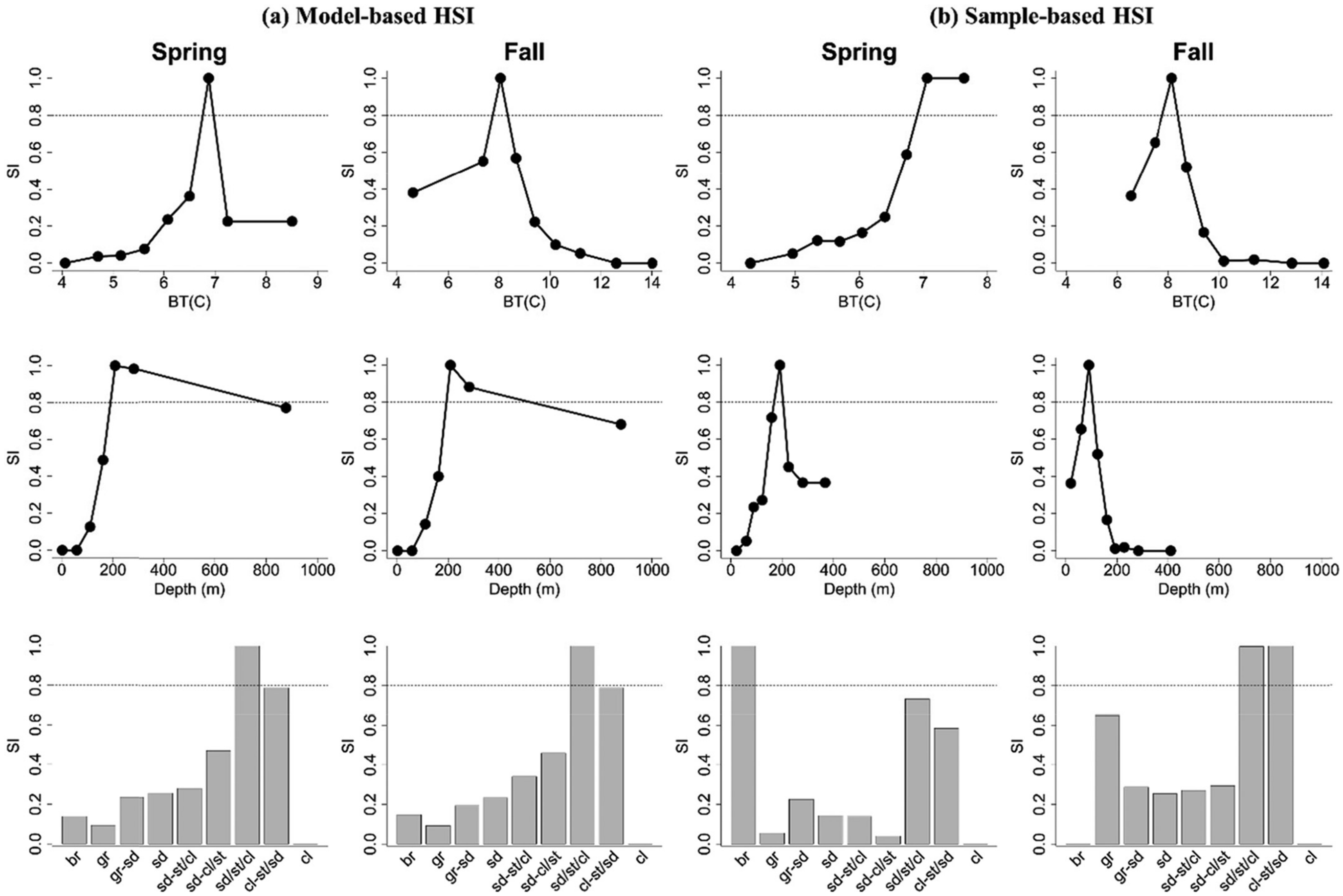

the BTS. Density-dependent processes cause systematic biases in BTS indices of abundance, which can lead to large errors in estimating species' spatial distribution (Thorson et al. 2013; Kotwicki et al. 2014). Density fields derived from both surveys have similar patterns in spatial distribution (i.e., high density versus low density) as those derived from the BTS only (Appendix A). However, there are finer resolution changes throughout the time series when the LLS is incorporated, particularly in fall. This qualitatively supports the hypothesis that cusk catches in the BTS have experienced density-dependent catchability. The LLS is thought to be a better method of sampling groundfish species that are not well sampled by mobile bottom tending gear (Hoey et al. 2013). Biases in predicting a species' spatial distribution can be addressed through the incorporation of data from surveys that sample habitats differently.

Accounting for differences in catchability has been shown to produce abundance estimates with reduced variability when multiple vessels are involved (Thorson and Ward 2014). The delta-GLMM (Thorson et al. 2015) estimated catchability for the LLS as well as before and after the 2009 protocol changes by considering these two time blocks to be surveys with separate catchability parameters. To test the sensitivity of the model to catchability estimates for the LLS, three different values of *b* were used to estimate area fished (i.e., 0.28, 0.56, 1.12 km; Appendix A). Varying values of area fished had no impact on the density estimates, and estimated catchability in the model accounted for differences in area fished (Appendix A). Finer temporal changes in catchability (e.g., year-specific changes) were not considered but may be useful to incorporate in the future or for species with similar circumstances. However, a random year effect was included to account for time-varying catchability for the BTS before and after 2009 and for the LLS.

Including the LLS when deriving density estimates changes the abundance estimates in the most recent years (Appendix A). As the LLS time series increases, the perceived systematic bias in abundance estimates from the BTS can be tested and addressed. The LLS would need to be conducted at the same locations as the BTS tows to compare catch rates from the two surveys to fully understand the consequences of spatially varying catchability (Thorson et al. 2013). As species decline and are more likely distributed in areas with a complex bottom, they become less accessible to trawl gear. Longline surveys can sample these areas to provide additional data complementary to the data derived in mobile trawl surveys. This study shows how data from longline and trawl gear can be combined within a modeling framework and how the HSI benefits from doing so.

HSI models

Overall, the model-based HSIs could better capture variance in abundance at different levels of habitat quality compared with sample-based HSIs. The increased spatial resolution of density estimates (Fig. 1) can provide information for a species' use of habitat without perfect sampling coverage or low catch rates. Utilizing model-based abundance indices changes the perception

Table 1. Habitat suitability indices (HSIs) model comparisons, showing linear regression results between abundance and arithmetic mean (AMM) and geometric mean (GMM) HSI results and Pearson's correlation coefficient (estimated in R).

Model	R^2	Correlation coefficient (r)	p value of t test for slope coefficient
Spring AMM, model-based HSI	0.384	0.619	<0.01
Without bottom temperature	0.266	0.516	<0.01
Without depth	0.362	0.602	<0.01
Without sediment	0.359	0.599	<0.01
Spring GMM, model-based HSI	0.437	0.661	<0.01
Without bottom temperature	0.280	0.529	<0.01
Without depth	0.419	0.647	<0.01
Without sediment	0.406	0.637	<0.01
Spring AMM, sample-based HSI	0.073	0.270	<0.01
Without bottom temperature	0.054	0.232	<0.01
Without depth	0.070	0.264	<0.01
Without sediment	0.060	0.245	<0.01
Spring GMM, sample-based HSI	0.085	0.291	<0.01
Without bottom temperature	0.058	0.241	<0.01
Without depth	0.083	0.288	<0.01
Without sediment	0.067	0.259	<0.01
Fall AMM, model-based HSI	0.293	0.541	<0.01
Without bottom temperature	0.262	0.512	<0.01
Without depth	0.219	0.468	<0.01
Without sediment	0.280	0.529	<0.01
Fall GMM, model-based HSI	0.304	0.551	<0.01
Without bottom temperature	0.280	0.529	<0.01
Without depth	0.222	0.471	<0.01
Without sediment	0.293	0.542	<0.01
Fall AMM, sample-based HSI	0.044	0.211	<0.01
Without bottom temperature	0.041	0.204	<0.01
Without depth	0.042	0.205	<0.01
Without sediment	0.032	0.179	<0.01
Fall GMM, sample-based HSI	0.039	0.199	<0.01
Without bottom temperature	0.038	0.194	<0.01
Without depth	0.043	0.208	<0.01
Without sediment	0.030	0.173	<0.01

of habitat use through two mechanisms. First, inclusion of the LLS provides data for the model outside of where the BTS sampled. The use of two gear types within the model-based density estimates provides increased data on habitat use because of the ability to sample in different sediment types. By utilizing all available data, the subsequent HSIs were better informed than both the sample-based HSIs and model-based HSIs that only used the BTS to predict abundance. Second, the estimated density fields by grid provides information where the LLS and (or) BTS did not sample. Increasing the spatial resolution of density estimates and the interaction with environmental variables is believed to be the primary driver in improving the HSIs.

Conventional sample-based HSIs are likely influenced by the availability of sampled data, as evidenced by the poor performance of sample-based HSIs relative to model-based HSIs (Table 1). The sampled depth ranges in spring (22–368 m) and fall (20–412 m) BTS limit what data are informing the HSI. Additionally, sampling frequency at various depths (Fig. 7) and sediment types (Fig. 6) influences the performance of HSIs. The limited data available for sample-based HSIs prompted the need for improving the spatial resolution of species' density estimates and environmental variables over a study area. The improved spatial resolution of environmental variables (i.e., per grid cell) overcomes the limitations of empirical data availability at a sampled location by providing finer-scale resolution of a species' interaction with these environmental variables. The improvements in spatial resolution also provide the ability to compare the overlap in habitat distribution of two species using the same spatial grid, a critical aspect of bycatch mitigation and species conservation.

However, the frequency of observations at each range within the environmental variables is influential on the HSI outcome. This was most notable for evaluating sediment type SIs. Sediment SIs for sample-based HSIs indicated bedrock to be the most important sediment type in the spring and a mixture of sand, clay, and silt in the fall (Fig. 4). A mixture of sand, silt, and clay was the most important sediment type for the spring and fall model-based HSIs, and bedrock was among the lowest (Fig. 4). The sample-based SI sediment curves are likely biased due to low catch rates in more complex sediment types (Fig. 6). Few cusk were caught in bedrock in the BTS (one in spring, zero in fall) and in gravel (two in spring and six in fall) between 1980 and 2013 (Fig. 6). The model-based HSIs provide abundance estimates for areas not directly observed in the survey, allowing for a different understanding of how cusk might be utilizing different sediment types. Model-based abundance estimates associated cusk with bedrock (20 times in the spring, 21 times in the fall) and gravel (95 times in the spring, 88 times in the fall). Cusk are thought to predominately reside on hard bottom (i.e., bedrock and gravel; Collette and Klein-MacPhee 2002), making the model-based abundance estimates associated with hard bottom more realistic with regard to presumed cusk behavior. The LLS could provide catch data for sediment types that the BTS cannot provide consistent data for, which provides more data for spatially explicit density estimates over the time series (Fig. 1). Model-based abundance estimates that incorporate the LLS are thought to improve data quality for use in habitat mapping by better informing the model in areas not well sampled by the BTS. However, the frequency of observations for both the sample-based and model-based HSIs are likely influencing the results.

Fig. 5. Habitat suitability index (HSI) maps for cusk. These HSI maps were derived from the model-based density estimates using data from both the bottom trawl survey (BTS) and longline survey (LLS). High habitat quality (red) is mostly offshore for both the spring and fall, and lower habitat quality (dark blue) is mostly inshore and around Georges Bank. Positive catch rates from the BTS (circles) and the LLS (triangles) are used to validate model predictions of cusk habitat quality. The size of the circle or triangle indicates catch rates, with smaller circles–triangles indicating lower catch rates compared with the larger circles–triangles. [Colour online.]

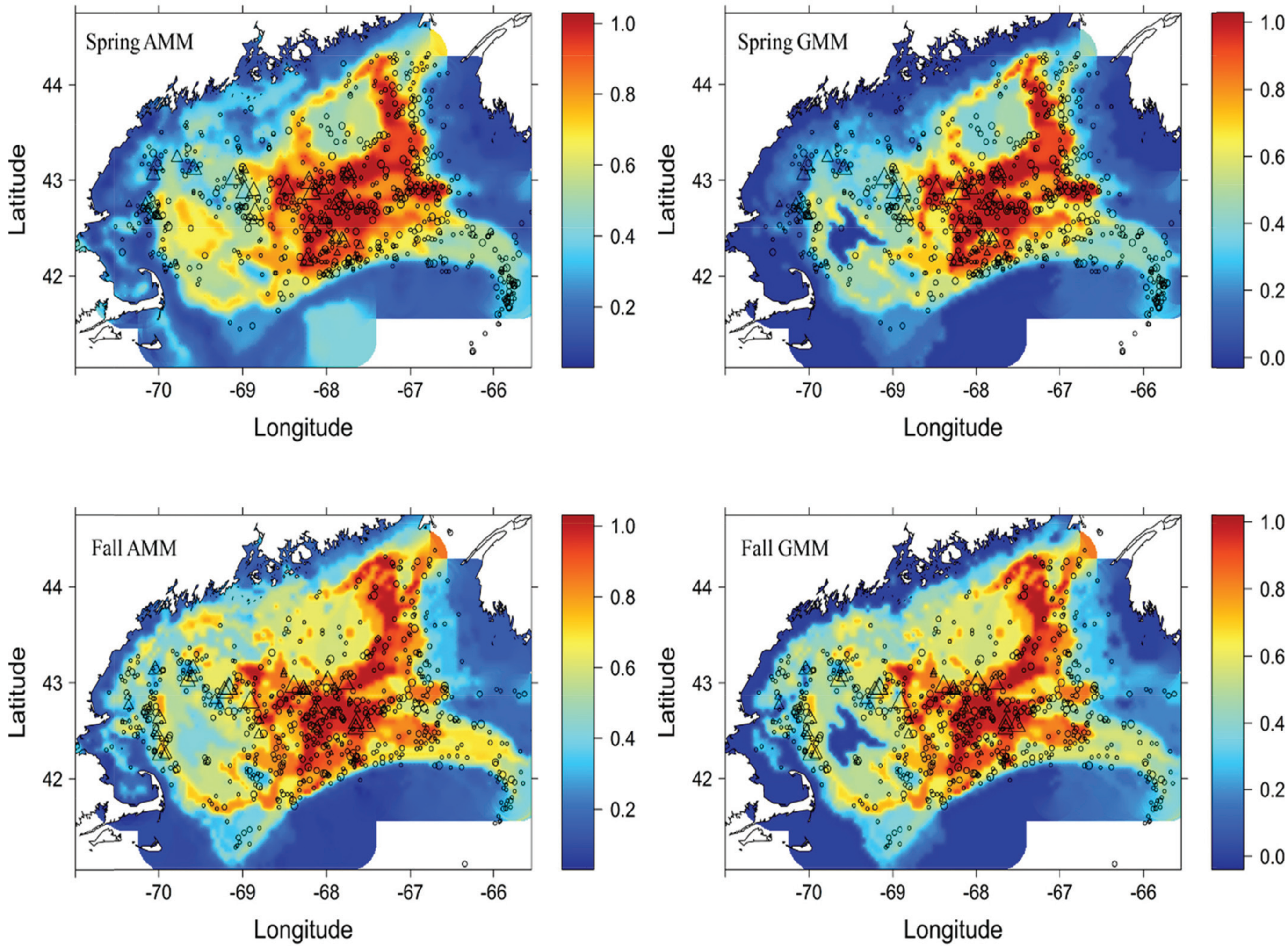

This study includes the three most important variables for this species reported in the literature (Collette and Klein-MacPhee 2002; Hare et al. 2012), reasonably capturing variability in habitat distribution with only three variables in the model-based HSIs. Temperature, depth, and sediment were equally weighted within the sample-based and model-based HSIs, and preliminary analyses indicated that SI weighting did not improve the HSIs. However, the relative contribution of each variable is likely not equal (Table 1). For model-based HSIs, temperature was the most influential variable in defining habitat suitability in spring while depth was the most influential in fall (Table 1). Temperature is hypothesized to be an important contributor to habitat suitability for cusk (Hare et al. 2012), but this evaluation indicates that variable importance may shift between seasons. However, mean seasonal temperatures and depth are positively correlated in the spring and negatively correlated in the fall, making it difficult to separate the relative influence of each variable. Even though depth and temperature are correlated, both variables contribute to defining habitat suitability (Table 1). Cusk spawn in the spring (Collette and Klein-MacPhee 2002) and may be seeking preferred temperatures in shallower waters during spawning events, while moving to deeper waters in the fall seeking colder temperatures.

Model limitations

HSI models are a relative index traditionally built from empirical data. These models cannot account for uncertainty in their estimates. Using model output as model input can incorporate unaccounted uncertainty that can be magnified within the second model (Brooks and Deroba 2015). However, the HSI model used in this study is not able to account for uncertainty no matter whether modeled or empirical data are used. Pearson residual plots indicate the incorporation of the LLS increased uncertainty due to the large differences in catch numbers between the two survey programs. HSIs assume that habitat suitability increases linearly with abundance. With limited data for sample-based HSIs, linear regressions were the most reliable method of testing model performance. Future research should focus on (1) building model-based HSIs with part of the data and using the remaining data to develop HSIs (Tanaka and Chen 2016); (2) using the delta-GLMM to evaluate habitat preference; and (or) (3) using model-based abundance estimates that have an associated uncertainty in abundance to account for uncertainty within habitat modeling.

This study did not assume that cusks' preferences for sediment, depth, and temperature change on an annual basis. The relationship between mean abundance and each of these variables was

Fig. 6. Spring and fall BTS positive catches of cusk by sediment type. Low catch rates of cusk at complex sediment types is likely to lead to biased sediment suitability index (SI) estimates. Sediment histograms are ordered from coarsest sediment (bedrock) to the finest sediment (clay). Sediment types include bedrock (br), gravel (gr), gravelly sediment (gr-sd), sand (sd), 33% sand, silt, and clay (sd/st/cl), 25%–50% sand with clay and silt (sd-cl/st), >75% sand with silt and clay (sd-st/cl), 50%–75% clay with silt with sand (cl-st/sd), and clay (cl) (Poppe et al. 2014).

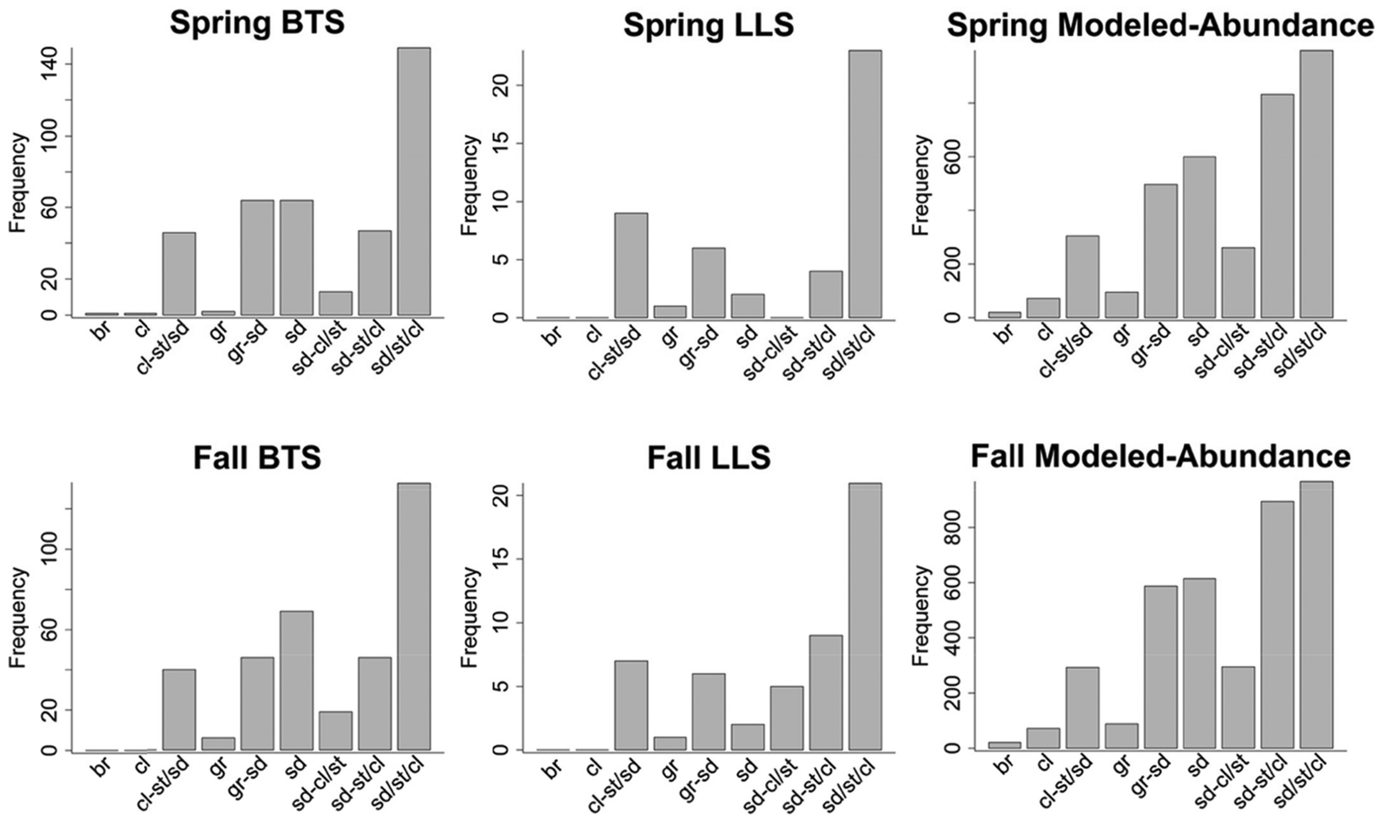

Fig. 7. Sampling frequency of depths in the NEFSC spring and fall bottom trawl surveys.

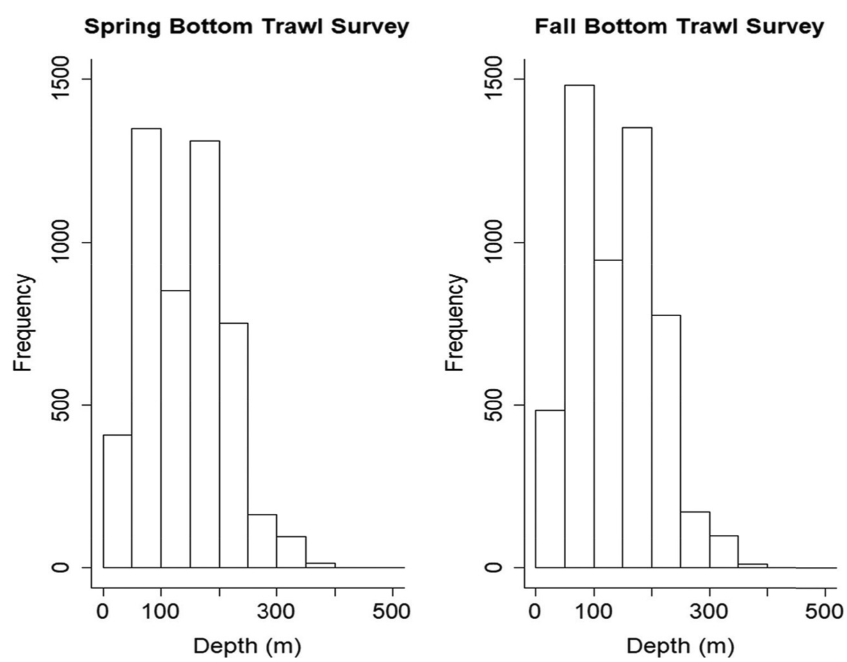

assumed to be constant during 1980 to 2013. HSI models are typically used for understanding a species' response to changes in habitat (Terrell and Carpenter 1997). Many HSI models assume that an organism's habitat preference does not change on an annual basis; distribution might, but the underlying relationship does not (Chen et al. 2011; Tanaka and Chen 2015; Guan et al. 2017). For the HSI models in this study to provide such insight, annual predictions would need to be made.

This study does not evaluate age- or size-dependent processes in habitat selection. Cusk caught in the LLS (2014–2015) have a simi-

Fig. 8. Size distribution of cusk caught in the NEFSC longline (2014–2015) and trawl surveys (1980–2015), spring and fall combined.

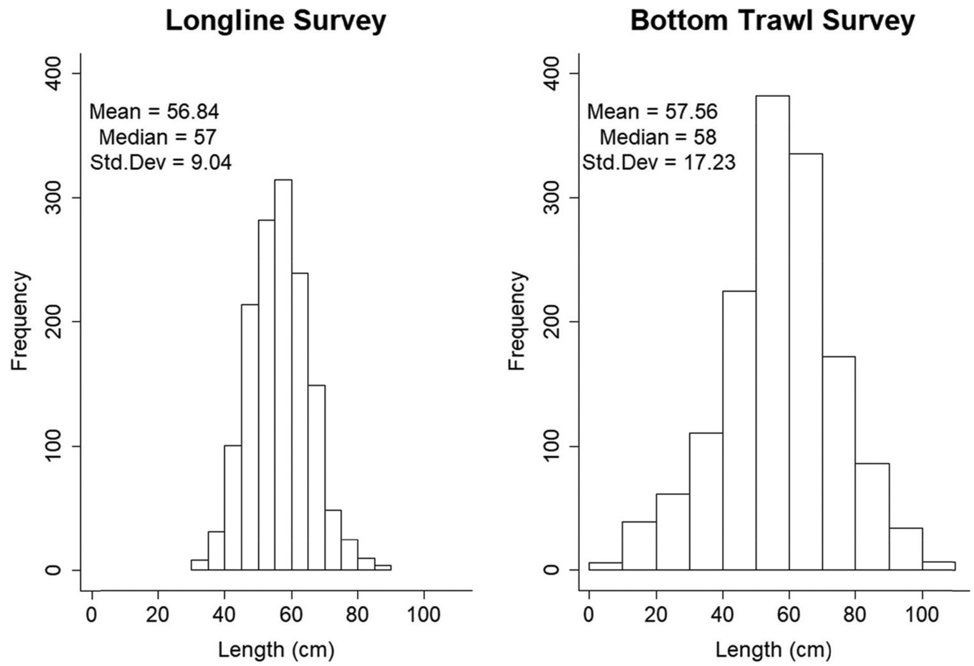

lar median size (57 cm) but narrower length range (30–84 cm) compared with cusk caught in the spring and fall BTS, which had a much wider length range (11–94 cm) but similar median size (58 cm). Cusk caught from 2014 to 2015 in the BTS have a smaller median size (50 cm) than cusk caught over the included time series (1980–2015) and in the LLS (Fig. 8). These size differences are expected given the two gear types have different selectivities; however, there are only 69 cusk caught in the BTS in 2014 and 2015. The mean size at maturity for cusk in the Scotian Shelf area is 50 cm for males and females combined (COSEWIC 2003). These two gear types catch predominantly mature individuals; a quarter of the catch is below 40 cm. Based on these size distributions, it is assumed that the habitat suitability indices represent adult habitat.

Annual density estimates can be used to build annual HSI models to evaluate how habitat quality has changed over a time series. The impacts of a changing climate can be better understood and predicted for the future by understanding the ideal range of each environmental variable. Currently, the delta-GLMM cannot predict potential or realized habitat (Grüss et al. 2017) as it can be from the HSI. However, several environmental factors influence a species' habitat use that might not be fully captured by the environmental variables used within an HSI. Even if all known environmental drivers were incorporated, there would likely be unaccounted for stochasticity within habitat distribution and species abundance. The spatiotemporal delta-GLMM captures spatial and spatial–temporal variability of species density through the random effects in the model (Thorson et al. 2015). The stochasticity of species distribution that is unlikely to be captured by any given variable or set of variables in the HSI is presumed to be captured by first predicting species density within the delta-GLMM. Environmental covariates incorporated into the delta-GLMM to predict species density could be used to evaluate the suitable range of environmental variables to understand species' habitat preferences as this model progresses.

Conclusion

The delta-GLMM provided a means of generating modeled abundance that reflects spatial heterogeneity in species density and utilizes all available survey data. The incorporation of different gear types to estimate abundance can, in part, overcome systematic density-dependent sampling biases that are seen in trawl surveys when a species' abundance contracts to habitat that is not effectively sampled by the survey. Spatially explicit abundance estimates provide a means of evaluating the habitat suitability by providing estimates in areas that were not directly sampled by the survey. The increased spatial resolution of abundance data improved the habitat suitability models in this study. A delta-GLMM offers a method of providing abundance information for areas not sampled by survey programs and for species caught in low numbers.

Acknowledgements

We thank James Thorson of the Northwest Fisheries Science Center for his reviews and help with the delta-GLMM. Thank you to the NEFSC internal reviewer for thoughtful comments for improving the second version of this manuscript. We thank the anonymous reviewer for the first version of this manuscript. We are grateful to Dave McLeroy at the NOAA NFSC for collecting the longline survey data. We also thank Nancy McHugh from the Ecosystems Surveys Branch, NOAA Fisheries, for providing the NEFSC bottom trawl survey data. We appreciate Kisei Tanaka of the University of Maine for his advice on habitat mapping. The NECOFS simulated temperature data in this study were from NERACOOS, Massachusetts Fishery Institution, and MIT Sea Grant College programs. This research was funded by NOAA Saltonstall–Kennedy grant number NOAA NA14NMF4270029.

References

Beardsley, R.C., Chen, C., and Xu, Q. 2013. Coastal flooding in Scituate (MA): a FVCOM study of the 27 December 2010 nor'easter. J. Geophys. Res. — Oceans, **118**: 6030–6045. doi:10.1002/2013JC008862.

Bivand, R. 2013. R Package "classInt": choose univariate class interval (Version 0.1-21) [online]. R-Project. Available at http://cran.r-project.org/web/packages/classInt/index.html [accessed 23 October 2014].

Brooks, E.N., and Deroba, J.J. 2015. When "data" are not data: the pitfalls of post hoc analyses that use stock assessment model output. Can. J. Fish. Aquat. Sci. **72**(4): 634–641. doi:10.1139/cjfas-2014-0231.

Brooks, R.P. 1997. Improving habitat suitability index models. Wildl. Soc. Bull. **25**(1): 163–167.

Brotons, L., Thuiller, W., Araujo, M.B., and Hirzel, A.H. 2004. Presence–absence versus presence-only modelling methods for predicting bird habitat suitability. Ecography, **27**: 437–448. doi:10.1111/j.0906-7590.2004.03764.x.

Chang, Y., Sun, C., Chen, Y., Yeh, S., and Dinardo, G. 2012. Habitat suitability analysis and identification of potential fishing grounds for swordfish, *Xiphias gladius*, in the South Atlantic Ocean. Int. J. Remote Sens. **33**(23): 7523–7541. doi:10.1080/01431161.2012.685980.

Chen, C., Beardsley, R.C., and Cowles, G. 2006. An unstructured grid, finite-volume coastal ocean model (FVCOM) system. Special Issue entitled "Advance in Computational Oceanography". Oceanography, **19**: 78–89. doi:10.5670/oceanog.2006.92.

Chen, X.J., Li, G., Feng, B., and Tian, S.Q. 2009. Habitat suitability of chub mackerel (*Scomber japonicus*) in the East China Sea. J. Oceanogr. **65**: 93–102.

Chen, X., Tian, S., Liu, B., and Chen, Y. 2011. Modeling a habitat suitability index for the eastern fall cohort of *Ommastrephes bartramii* in the central North Pacific Ocean. Chin. J. Ocean. Limnol. **29**(3): 493–504. doi:10.1007/s00343-011-0058-y.

Cohen, D.M., Inada, T., Iwamoto, T., and Scialabba, N. 1990. Gadiform fishes of the world. Food and Agriculture Organization of the United Nations Species Catalogue. Fir/S125. Vol. 10.

Collette, B.B., and Klein-MacPhee, G. 2002. Bigelow and Schroeder's fishes of the Gulf of Maine. Smithsonian Institution, Washington, D.C.

COSEWIC. 2003. Assessment and Status Report on the Cusk (*Brosme brosme*) in Canada. May 2003. Committee on the Status of Endangered Wildlife in Canada.

Davies, T.D., and Jonsen, I.D. 2011. Identifying nonproportionality of fishery-independent survey data to estimate population trends and assess recovery potential for cusk (*Brosme brosme*). Can. J. Fish. Aquat. Sci. **68**(3): 413–425. doi:10.1139/F10-165.

GEBCO. 2014. The GEBCO_2014 Grid, version 20150318 [online]. Available from http://www.gebco.net. General Bathymetric Chart of the Oceans.

Grüss, A., Thorson, J.T., Sagarese, S.R., Babcock, E.A., Karnauskas, M., Walter, J.F., III, and Drexler, M. 2017. Ontogenetic spatial distributions of red grouper (*Epinephelus morio*) and gag grouper (*Mycteroperca microlepis*) in the Northern Gulf of Mexico. Fish. Res. **193**: 129–142. doi:10.1016/j.fishres.2017.04.006.

Guan, L., Chen, Y., and Wilson, J.A. 2017. Evaluating spatio-temporal variability in the habitat quality of Atlantic cod (*Gadus morhua*) in the Gulf of Maine. Fish. Oceanogr. **26**(1): 83–96. doi:10.1111/fog.12188.

Hare, J.A., Manderson, J.P., Nye, J.A., Alexander, M.A., Auster, P.J., Borggaard, D.L., Capotondi, A.M., Damon-Randall, K.B., Heupel, E., Mateo, I., O'Brien, L., Richardson, D.E., Stock, C.A., and Biegel, S.T. 2012. Cusk (*Brosme brosme*) and climate change: assessing the threat to a candidate marine fish species under the US Endangered Species Act. ICES J. Mar. Sci. **69**(10): 1753–1768. doi:10.1093/icesjms/fss160.

Hoey, J., O'Brien, L., Natanson, L., McMlroy, D., Manderson, J., Borggaard, D., and Silva, R. 2013. Development of a bottom longline survey for stocks associated with complex rocky habitat in the western and central Gulf of Maine, including several data poor stocks that are ESA species of concern. NEFSC & NERO PROPOSAL 2013 Cooperative Research Solicitation. Available from National Marine Fisheries Service, 166 Water Street, Woods Hole, MA 02543-1026, USA.

Kotwicki, S., Ianelli, J.N., and Punt, A.E. 2014. Correcting density-dependent effects in abundance estimates from bottom trawl surveys. ICES J. Mar. Sci. **71**: 1107–1116. doi:10.1093/icesjms/fst208.

Løkkeborg, S., Olla, B.L., Pearson, W.H., and Davis, M.W. 1995. Behavioural responses of sablefish, *Anoplopoma fimbria*, to bait odour. J. Fish Biol. **46**: 142–155. doi:10.1111/j.1095-8649.1995.tb05953.x.

MacCall, A.D. 1990. Dynamic geography of marine fish populations. University of Washington Press, Seattle, Wash., USA.

Miller, T.J., Das, C., Politis, P.J., Miller, A.S., Lucey, S.M., Legault, C.M., Brown, R.W., and Rago, P.J. 2010. Estimation of *Albatross IV* to *Henry B. Bigelow* calibration factors. Northeast Fish Sci. Cent. Ref. Doc. 10-05. Available from National Marine Fisheries Service, 166 Water Street, Woods Hole, MA 02543-1026, USA.

Morris, L., and Ball, D. 2006. Habitat suitability modelling of economically important fish species with commercial fisheries data. ICES J. Mar. Sci. **63**(9): 1590–1603. doi:10.1016/j.icesjms.2006.06.008.

NECOFS. 2013. Northeast Coastal Ocean Forecasting System Main Portal [online]. Available from http://fvcom.smast.umassd.edu/research_projects/NECOFS.

NEFSC. 2013. 55th Northeast Regional Stock Assessment Workshop (55th SAW) Assessment Report. US Dept. Commer., Northeast Fish. Sci. Cent. Ref. Doc. 13-11. Available from National Marine Fisheries Service, 166 Water Street, Woods Hole, MA 02543-1026, USA, or online from http://www.nefsc.noaa.gov/nefsc/publications/. Northeast Fisheries Science Center.

Politis, P.J., Galbraith, J.K., Kostovick, P., and Brown, R.W. 2014. Northeast Fisheries Science Center Bottom Trawl Survey Protocols for the NOAA Ship *Henry B. Bigelow*.

Poppe, L.J., McMullen, K.Y., Williams, S.J., and Paskevich, V.F. (*Editors*). 2014. USGS east-coast sediment analysis: Procedures, database, and GIS data (ver. 3.0, November 2014) [online]. US Geological Survey Open-File Report 2005-1001. Available from http://pubs.usgs.gov/of/2005/1001/.

Schnute, J.T., Boers, N., and Haigh, R. 2015. Mapping fisheries data and spatial analysis tools. R package. Fisheries and Oceans Canada.

Tanaka, K., and Chen, Y. 2015. Spatiotemporal variability of suitable habitat for American lobster (*Homarus Americanus*) in Long Island Sound. J. Shellfish Res. **34**(2): 531–543. doi:10.2983/035.034.0238.

Tanaka, K., and Chen, Y. 2016. Modeling spatiotemporal variability of the bioclimate envelope of *Homarus americanus* in the coastal waters of Maine and New Hampshire. Fish. Res. **177**: 137–152. doi:10.1016/j.fishres.2016.01.010.

Terrell, J.W. 1984. Proceedings of a workshop on fish habitat suitability index models. Biological Report Vol. 85.

Terrell, J.W., and Carpenter, J. 1997. Selected habitat suitability index model evaluations. Information and Technology Report, USGS/BDR/IT — 1997-0005.

Thorson, J.T. 2017. VAST user manual [online]. Available from https://github.com/James-Thorson/VAST [accessed 19 May 2017].

Thorson, J.T., and Barnett, L.A.K. 2017. Comparing estimates of abundance trends and distribution shifts using single- and multispecies models of fishes and biogenic habitat. ICES J. Mar. Sci. **74**(5): 1311–1321.

Thorson, J.T., and Ward, E.J. 2014. Accounting for vessel effects when standardizing catch rates from cooperative surveys. Fish. Res. **155**: 168–176. doi:10.1016/j.fishres.2014.02.036.

Thorson, J.T., Clarke, M.E., Stewart, I.J., and Punt, A.E. 2013. The implications of spatially varying catchability on bottom trawl surveys of fish abundance: a proposed solution involving underwater vehicles. Can. J. Fish. Aquat. Sci. **70**(2): 294–306. doi:10.1139/cjfas-2012-0330.

Thorson, J.T., Shelton, A.O., Ward, E.J., and Skaug, H.J. 2015. Geostatistical delta-generalized linear mixed models improve precision for estimated abundance indices for West Coast groundfishes. ICES J. Mar. Sci. **72**(5): 1297–1310. doi:10.1093/icesjms/fsu243.

Yu, W., Qian, Y., Chen, X., and Chen, Y. 2016. Modelling the effects of climate variability on habitat suitability of jumbo flying squid, *Dosidicus gigas*, in the Southeast Pacific off Peru. ICES J. Mar. Sci. **73**(2): 239–24. doi:10.1093/icesjms/fsv223.

Zhou, S., Klaer, N.L., Daley, R.M., Zhu, Z., Fuller, M., and Smith, A.D.M. 2014. Modelling multiple fishing gear efficiencies and abundance for aggregated populations using fishery or survey data. ICES J. Mar. Sci. **71**(9): 2436–2447. doi:10.1093/icesjms/fsu068.

Appendix A. Developing density estimates and abundance indices utilizing multiple gear types

This study, in part, set out to determine if data from two different gear types could be combined to develop indices of abundance for data-limited species using the delta-GLMM. Positive catch rates in the model are a function of area swept. However, this study combined two types of surveys with two different concepts of "area swept". The bottom trawl survey (BTS) area swept is considered a standardized volume that is a function of the width of the doors and trawl speed. Longline surveys (LLSs) do not have a standardized area fished.

The delta-GLMM first estimates the probability of presence, then estimates positive catch rates in the second stage. The first and second stages of the model are fit using the survey data. The first stage of the model is fit as a function of annual mean density, catchability, and spatial and spatial temporal random effects estimated from the nearest knot. The second stage of the model is fit given all of the same parameters as a function of area swept. Catchability is then removed, and the underlying species density is predicted at each knot. Total abundance across the domain is calculated as follows:

$$\text{(A.1)}\qquad \hat{b}_t = \sum_{j=1}^{n_j} a_j \operatorname{logit}^{-1}\left[d^{(p)}_{T_{(i)}} + \omega^{(p)}_{J_{(i)}} + \varepsilon^{(p)}_{J_{(i)},T_{(i)}}\right] \times \exp\left[d^{(\lambda)}_{T_{(i)}} + \omega^{(\lambda)}_{J_{(i)}} + \varepsilon^{(\lambda)}_{J_{(i)},T_{(i)}}\right]$$

Full model details can be found in Thorson et al. (2015).

To test if catchability within the delta-GLMM was capable of accounting for differences of gear types, different estimates of area fished were evaluated for the LLS. The distance between the beginning and end of a longline set were known, but the bait plume around the longline was not known. Bait plume is a function of current speed and direction, bait type, and soak duration, which sets the range over which the bait can be detected, as well as factors influencing the range over which fish will respond to detected bait; the fish response factors include length of food deprivation (i.e., hunger), fish size, and swimming speed (Løkkeborg et al. 1995; Zhou et al. 2014). These specifics are not known in fisheries surveys, and feeding response to bait plumes has not been measured for cusk. Without knowing the details necessary to estimate the bait plume, three values of b were tested based on

Fig. A1. *Brosme brosme* model-based abundance indices, derived from the both the NEFSC bottom trawl survey and longline survey combined and the NEFSC bottom trawl survey only. The spring and fall model-based abundance indices accounted for spatial and spatiotemporal randomness. Error bars are standard deviations from the annual mean. [Colour online.]

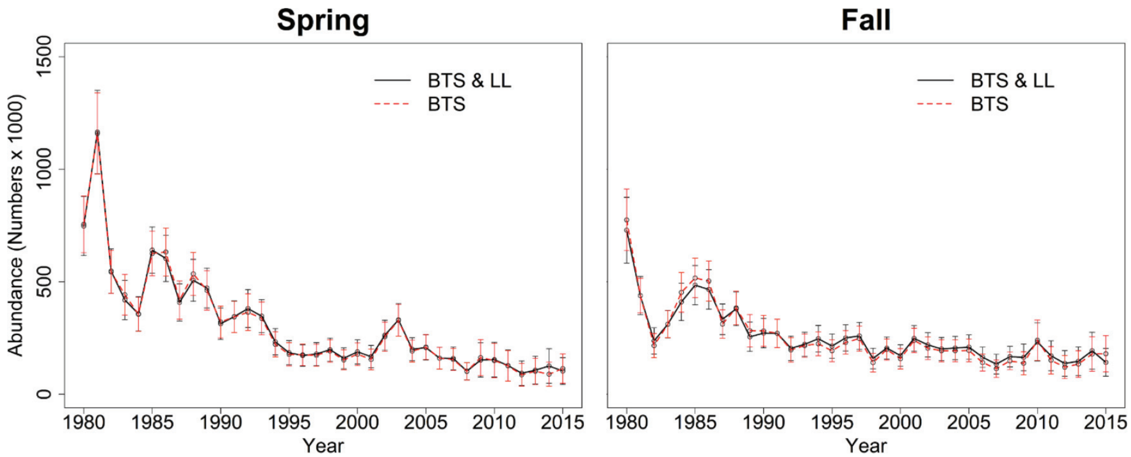

the estimates for moderate food deprivation in Løkkeborg et al. (1995). A minimum, medium, and maximum value of *b* (0.28, 0.56, and 1.12 km, respectively) were used to test the sensitivity of abundance estimates to longline area fished.

A total of six model-based density fields with different configurations of values for *b* were estimated for spring and fall. Each season had three models that incorporated both the BTS and LLS using the three values of *b* (i.e., 0.28, 0.56, and 1.12 km). The resulting estimates for area fished varied by an order of magnitude (less than 0.5 km^2 when b = 0.28 km and up to 2.0 km^2 when b = 1.121 km). Three catchability parameters were estimated to account for the 2009 protocol changes in the BTS. The estimated abundance index for the three models in the spring and three in the fall were unchanged with changes in the value of *b*. Akaike information criteria values (AICs) for all three values of *b* were unchanged for the different model runs in both the spring (3837) and the fall (3676).

Four model-based abundance indices were derived using only the spring and fall BTS then combining the BTS and the spring and fall LLS. Two catchability coefficients were defined for before and after the 2009 protocol changes to the BTS, treating the survey as two surveys within each season with no temporal overlap. Therefore, models with data from both survey programs estimated three catchability parameters, and models that included only the BTS estimated two parameters. The resulting abundance estimates do not vary in relative trend from the abundance estimates using the combined surveys (Fig. A1). Abundance was high in 1980–1981, with a decline to persistent low levels since 2005 (Fig. A1). However, there is a slight difference in trends for the two most recent years of the time series (2014–2015) when the longline survey is added (Fig. A1). All model-based abundance indices show a decrease in cusk abundance over the time series (1980–2015) for both seasons. Pearson residual plots suggest there is no significant spatiotemporal pattern in the residuals (Fig. A2).

When catchability was not estimated for the LLS, the annual abundance index was inconsistent and highly variable during the exploratory phase of this study (results not shown). The delta-GLMM could account for differences in catchability between the LLS and BTS, indicating this is an effective method of incorporating multiple surveys with different gear types to estimate abundance indices, even without accurate bait plume measures for a longline survey.

Fig. A2. (Upper panels) Density field plots from the delta-generalized spatiotemporal model. Red indicates areas of higher abundance; blue indicates areas of lower abundance. (Lower panels) Pearson residual plots of the density field estimates from the delta-generalized spatiotemporal model. [Colour online.]